JOURNAL OF CATALYSIS **57**, 153–166 (1979)

X-Ray Photoelectron Spectroscopy Study of Cobalt–Molybdenum Binary Oxide Catalysts

YASUAKI OKAMOTO, TAKAFUMI SHIMOKAWA, TOSHINOBU IMANAKA,
AND SHIICHIRO TERANISHI

*Department of Chemical Engineering, Faculty of Engineering Science,
Osaka University, Toyonaka, Osaka 560 Japan*

Received June 6, 1978; revised November 13, 1978

The surface compositions of cobalt–molybdenum binary oxide catalysts were studied with X-ray photoelectron spectroscopic techniques for the calcined catalysts and for the catalysts exposed to various reactive gases relating to the hydrodesulfurization of thiophene. In the cases of the cobalt–molybdenum catalysts prepared by calcining the mixtures of cobalt nitrate and ammonium paramolybdate, a surface segregation of molybdenum was observed over a wide range of the bulk composition of the catalyst, while a cobalt enrichment was observed in the catalyst with a small cobalt content (<6 at.%). However, the catalysts prepared by the calcination of the mixed composite oxides, CoO and MoO_3, showed no enrichment of cobalt or molybdenum in the catalyst surface, except for the catalyst containing a small amount of CoO. It was found that the surface composition of the catalyst was changed considerably by treating at 400°C with 10 Torr of various reactive gases. Hydrogen reduction caused a surface enrichment of molybdenum, accompanied by the reduction of both oxides to MoO_2 and Co metal. Thiophene/H_2 also resulted in a surface segregation of molybdenum and the sulfidation of MoO_2 to MoS_2. H_2S/H_2 treatments, on the other hand, produced a drastic segregation of cobalt in the catalyst surface and sulfided the catalyst completely to form MoS_2 and CoS and/or more likely Co_9S_8, together with excess sulfur. A similar behavior was observed for a zinc–molybdenum binary oxide catalyst. It is concluded that the surface compositions of the cobalt–molybdenum catalysts depend strongly on the preparation procedures and on the kinds of gases in contact with the catalysts.

INTRODUCTION

It is well known that surface and bulk compositions are different in the cases of bimetallic alloys and that a preferential enrichment of one component of a binary alloy occurs when the alloy is exposed to reactive gases (*1*, *2*). However, in the cases of multicomponent oxide catalysts, only little evidence was presented on the differences between surface and bulk compositions, although such behavior can be expected similarly for the oxide catalysts on the basis of thermodynamical considerations (*3*).

Matsuura and Wolfs (*4*) have reported the differences between surface and bulk compositions for multicomponent bismuth–molybdate catalysts. The decrease in surface concentration of bismuth has been noted for bismuth–molybdate catalysts when they are reduced in hydrogen (*5*) and the increased intensities of XPS (X-ray photoelectron spectroscopy or ESCA) spectra of Mo, Bi, and Fe have been observed after ammoxidation of propylene for a silica-supported multicomponent bismuth–molybdate catalyst (*6*). Very recently, Okamoto and his co-workers have demon-

0021-9517/79/040153-14$02.00/0

strated with SnO_2–MoO_3 binary oxide catalysts that the surface composition is remarkably different from the bulk one and that the catalytic activities for the dehydration and oxidative dehydrogenation of *s*-butanol depend on the surface composition of the catalyst during the reaction but not on the bulk composition (*7*). These findings suggest the importance in defining the surface compositions of oxide catalysts under reaction conditions, coupled with the chemical state of each catalyst component, since catalytic reactions take place on the catalyst surfaces.

In this paper, the changes in the surface compositions of cobalt–molybdenum binary oxide catalysts were studied with XPS techniques during a variety of treatments relating to the hydrodesulfurization of thiophene, together with the differences between surface and bulk compositions of the calcined catalysts. It is revealed that the surface compositions are markedly dependent on the preparation methods and treatments even in the binary oxide catalysts. Moreover, it is strongly suggested that much more attention should be paid to the surface compositions of catalysts in order to discuss the catalytic properties in detail.

EXPERIMENTAL METHODS

Materials

Cobalt–molybdenum binary oxide catalysts with various compositions were prepared by two methods: Co–Mo (A) catalysts: ammonium paramolybdate and cobaltous nitrate were dissolved simultaneously in hot water and evaporated to dryness under vigorous stirring, followed by a calcination in air at 550°C for 5 hr using an electric furnace independent from an XPS equipment; and Co–Mo (B) catalysts: CoO and MoO_3 (both were supplied in fine powder forms by Nakarai Chemical Company) were mixed completely using a motar in the presence of a small amount of water and then dryed at 110°C for 16 hr with a subsequent calcination at 550°C for 5 hr. Both catalysts were obtained in fine powders after the calcination. Preparation methods similar to the Co–Mo (A) catalysts were employed for zinc–molybdenum binary oxide catalysts by using zinc nitrate instead of cobaltous nitrate. Cobalt–alumina catalysts (10 and 20 wt% CoO) were prepared by impregnating cobaltous nitrate on γ-alumina (BET surface area; 213 m^2/g), subsequently calcined at 550°C for 5 hr.

The treatment gases used in this study were H_2, thiophene/H_2, H_2S/H_2, thiophene/H_2S/H_2, H_2S, thiophene vapor, and O_2. Their compositions were 1/15 for thiophene/H_2 and H_2S/H_2 and 1/1/15 for thiophene/H_2S/H_2.

Procedures

XPS spectra were recorded on a Hitachi 507 spectrometer by using $\mathrm{Al}K\alpha_{1,2}$ radiation at room temperature as reported previously (*8*). A catalyst powder was mounted onto a grid attached to a sample holder made of stainless steel. All binding energies were referenced to the contaminant carbon (C 1*s* = 285.0 eV). Ten Torr (1 Torr = 133.3 N m^{-2}) of various gases were introduced into a sample pretreatment chamber attached to the spectrometer at 20 min intervals, followed by evacuation before a subsequent admission of a treatment gas. The catalyst was maintained at 400°C during treatments and cooled down to room temperature for recording XPS spectra. The base pressure in the analyzing chamber was about 1×10^{-7} Torr.

In order to estimate atomic ratios ((Co/Mo) and (S/Mo)) from XPS peak area intensities, the XPS spectra of Mo 3*d*, S 2*p*, and Co $2p_{\frac{3}{2}}$ levels for MoS_2 and $CoSO_4$ were measured several times as standard compounds. In the cases of zinc–molybdate catalysts, MoS_2 and $ZnSO_4$ were employed for the sake of calibration, in which Zn $2p_{\frac{3}{2}}$ level was used. In the above calibration methods, the effect of contaminant carbon

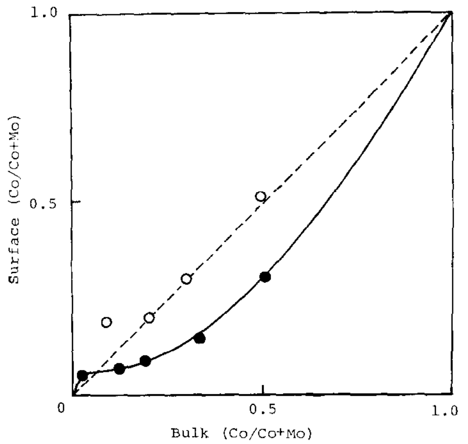

FIG. 1. Correlations between surface and bulk compositions of the Co–Mo binary oxide catalysts; ●, Co–Mo(A); ○, Co–Mo(B). Dashed line indicates the correlation to show the same composition as the bulk one.

was neglected, because C 1*s* intensities were almost invariant among the standard compounds and the catalysts.

Diffuse reflectance spectra of the Co–Mo catalysts were recorded in the range 200 to 800 nm by use of Hitachi 200-20 spectrophotometer against standards of alumina.

RESULTS AND DISCUSSION

1. Surface Composition of Calcined Catalysts

The surface compositions of the two series of the Co–Mo binary oxide catalysts, the Co–Mo (A) and (B), were compared with the bulk compositions in Fig. 1. A considerable superficial enrichment of molybdenum in the Co–Mo (A) catalyst was observed except below a small content of cobalt (Co/Co + Mo < 0.06). The XPS spectra of Mo 3*d* and Co $2p_{3/2}$ levels (Figs. 2a and 3a) show molybdenum as MoO_3 and/or $CoMoO_4$ (Mo $3d_{5/2}$: 233.2 eV) and a large portion of cobalt as Co^{2+} (Co $2p_{3/2}$: 781.9 eV; spin–orbit splitting: ca. 16 eV; and the presence of satellite peak (*9*, *10*)) in the all Co–Mo catalysts (Co/Co + Mo < 0.5) studied in this work after the calcination. The diffuse reflectance spectra of the calcined catalysts indicated that a significant amount of cobalt exists as α-$CoMoO_4$ (527 and 585 nm) and the remainder as cobalt oxide (750 nm). Taking into account these facts, it appears that a considerable portion of cobalt exists as $CoMoO_4$ (Co^{2+}) in the catalyst surface and that the remaining one as cobalt oxide (probably as Co_3O_4 (*11*)). The surface segregation of molybdenum in the Co–Mo catalysts will result from the smaller surface free energy of MoO_3 (50–70 ergs/cm^2) than that of Co_3O_4, which surface free energy can be estimated to be 500 to 1000 ergs/cm^2 (*3*) and probably smaller than that of $CoMoO_4$. However, the slight cobalt enrichment observed in the low cobalt content catalyst might be due to the exclusion of cobalt from the bulk of the catalyst by the crystallization of MoO_3. Nevertheless, as shown in Fig. 1, no en-

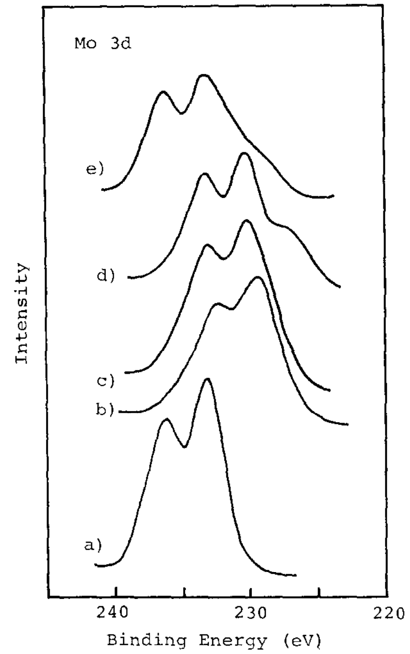

FIG. 2. XPS spectra of the Mo 3*d* level for the Co–Mo(B) catalyst containing 30 at.% of cobalt; (a) after calcination at 550°C for 5 hr, (b) after reduction at 400°C with H_2 for 100 min (Fig. 5), (c) after subsequent exposure to thiophene/H_2 at 400°C for 60 min (Fig. 5), (d) to H_2S/H_2 at 400°C for 100 min (Fig. 5), and (e) to thiophene vapor at 400°C for 60 min.

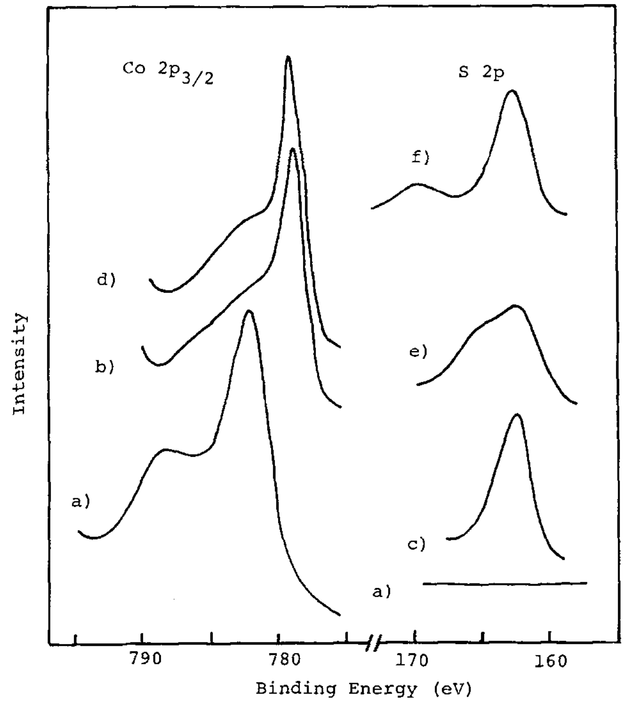

FIG. 3. XPS spectra of the Co $2p_{3/2}$ and S $2p$ levels for the Co–Mo(B) catalyst (30 at.% of cobalt); (a)–(e) see captions in Fig. 2; (f) after O_2 treatment of the sulfided catalyst at 400°C for 30 min (Fig. 6).

richment of molybdenum or cobalt was detected for the Co–Mo (B) catalysts. This is probably due to the deficiency of a thermodynamical equilibrium under our preparation conditions. It is revealed that the surface compositions of the Co–Mo catalysts depend strongly on the preparation methods employed.

According to Canesson *et al.* (*12*), no signal of cobalt was detected with XPS, contrary to our results, for MoS_2 catalysts doped with a small amount of Co_9S_8 ($Co/Co + Mo < 0.05$). This discrepancy will result from the different systems examined. However, an abnormal enrichment of a dopant with small concentration was also found for a SnO_2–ZrO_2 catalyst system, where SnO_2 was excluded from the bulk to the catalyst surface in a small concentration range of SnO_2, while the surface concentration of SnO_2 was depressed in the wide range of the bulk composition of the catalyst (*13*). With regard to Co_3O_4 catalysts doped with a small amount of Al_2O_3 or MgO, ISS (ion scattering spectroscopy) shows the superficial enrichments of Al_2O_3 and probably of MgO (*14*). On the other hand, no surface segrega-

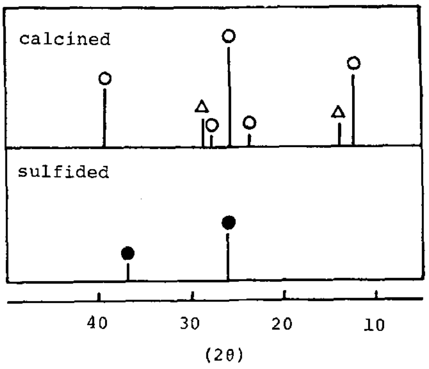

FIG. 4. X-ray diffraction patterns of calcined (upper) and sulfided (lower) Co–Mo(B) catalysts (Co: 30 at.%); ○, MoO_3, △, α-$CoMoO_4$; ●, MoO_2.

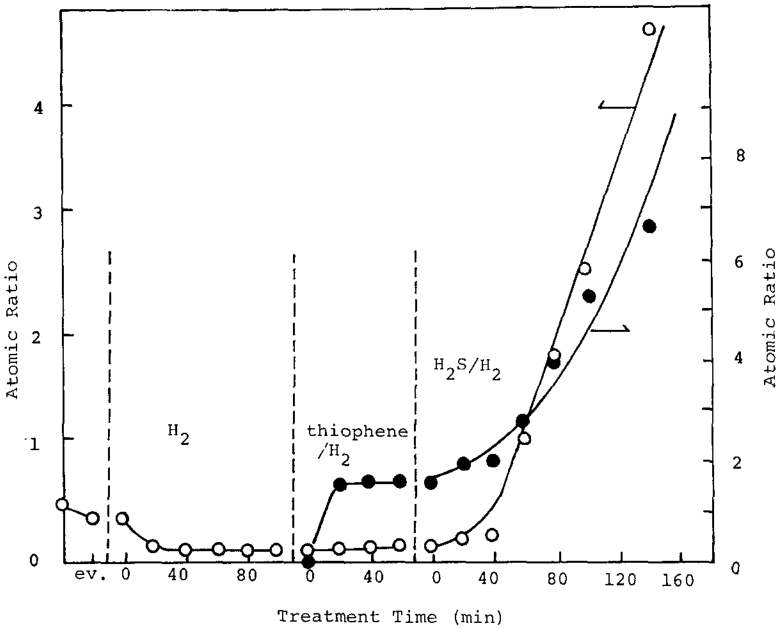

FIG. 5. Surface composition and sulfur content of the Co–Mo (B) catalyst (Co: 30 at.%) during consecutive treatments at 400°C with 10 Torr of gases at 20 min intervals; evacuation, H_2, thiophene/H_2, and H_2S/H_2; ○, (Co/Mo), ●, (S/Mo).

tion of SiO_2 or Al_2O_3 has been detected for SiO_2–Al_2O_3 catalysts (*15*). Consequently, these findings suggest that the surface composition of a catalyst depends considerably on the preparation methods and on the kinds of composite oxides even in the cases of oxide catalysts and, therefore, that the surface concentration of each catalyst component should be defined by appropriate techniques in order to discuss catalytic properties in detail, as suggested recently by Okamoto *et al.* (*7*).

2. Changes in Surface Composition during Various Treatments

The Co–Mo binary oxide catalysts were exposed to various gases relating to the hydrodesulfurization of thiophene. In the following studies, the Co–Mo (B) catalyst with the composition of Co/Co + Mo = 0.3 was used since the best activities for various reactions including the hydrodesulfurization of thiophene have been reported for the catalysts with such compositions in the cases of MoS_2–Co_9S_8 catalysts (*12, 16*). With the Co–Mo (A) catalysts, similar results were confirmed.

The X-ray diffraction pattern (Cu*Kα*) of the catalyst was examined to reveal the bulk structure. As shown in Fig. 4, the catalyst consists of MoO_3 and α-$CoMoO_4$, in agreement with the diffuse reflectance spectra. However, the presence of a small amount of cobalt oxide cannot be ruled out because of its intrinsic weak intensity.

In Fig. 5, the (Co/Mo) and (S/Mo) atomic ratios, which were obtained from XPS intensity ratios by using the relative atomic sensitivities, are shown for the successive treatments with 10 Torr of H_2, thiophene/H_2, and H_2S/H_2. The catalyst was brought in the repeated contacts with these gases at 400°C. The XPS spectra of Mo $3d$, Co $2p_{3/2}$, and S $2p$ levels are shown in Figs. 2 and 3a–d after the treatments.

After evacuation at 400°C for 1 hr, some molybdenum was reduced with a slight decrease in the (Co/Mo) ratio. The introduction of H_2 caused the rapid reduction of the catalyst to form MoO_2 (Mo $3d_{5/2}$: 229.5 eV) and Co metal (Co $2p_{3/2}$: 778.7 eV) as are shown in Figs. 2b and 3b. After 20 to 40 min, the catalyst was almost completely reduced to MoO_2 and Co metal, accompanied by a further decrease in the (Co/Mo) ratio to one-fifth of that for the calcined catalyst. When the catalyst was exposed to thiophene/H_2 after the H_2 reduction, no significant change in the (Co/Mo) ratio was observed, while the sulfur content of the catalyst, (S/Mo), reached a constant value after 20 min with a chemical shift of 0.7 eV in the Mo $3d_{5/2}$ level (Fig. 2c) and without any shift in the Co $2p_{3/2}$ level. The (S/Mo) atomic ratio was 1.8 after 60 min and the binding energy of Mo $3d_{5/2}$ was 230.2 eV, which was consistent with that for MoS_2. In addition, it was confirmed that Co metal was sulfided to a much less extent when treated with thiophene/H_2 under similar conditions. Therefore, it is evident that MoO_2 is preferentially sulfided to MoS_2 and Co metal is not virtually sulfided by the treatments with 10 Torr of thiophene/H_2 at 400°C. Following the exposure to thiophene/H_2, the catalyst was repeatedly brought in contact with H_2S/H_2. As shown in Fig. 5, the (Co/Mo) ratio increased drastically with a great increase in the sulfur content of the catalyst. These findings clearly indicate that an enormous enrichment of cobalt in the catalyst surface occurs by the contact with H_2S/H_2 and that cobalt is sulfided. The Co $2p_{3/2}$ spectrum in Fig. 3d shows a slight positive chemical shift (ca. 0.4 eV) compared to the binding energy for Co metal. The observed shift is considered to indicate the sulfidation of cobalt, since the binding energy of the Co $2p_{3/2}$ level for CoS has been reported to have 2.4 eV lower binding energy than that for CoO (*9*) in agreement with the observed shift. The

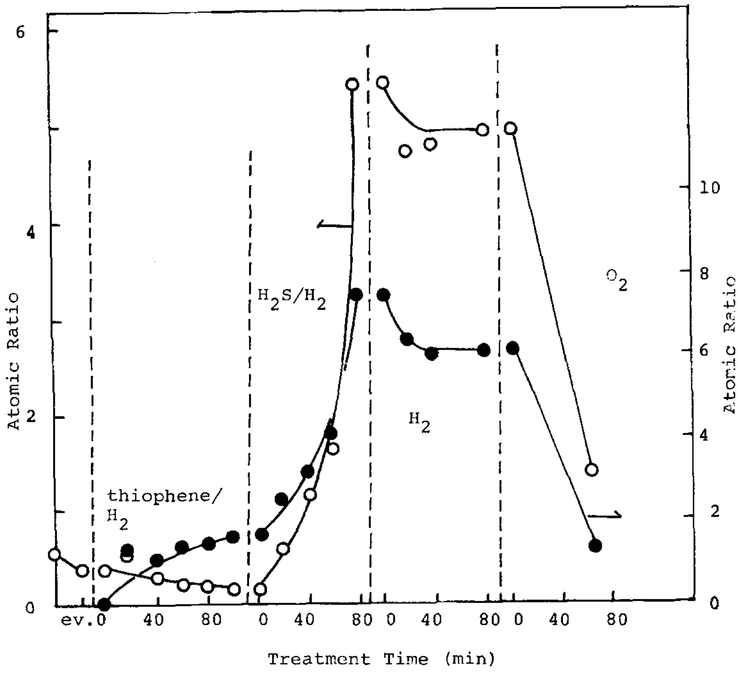

FIG. 6. Surface composition and sulfur content of the Co–Mo (B) catalyst (Co: 30 at.%) during treatments at 400°C; evacuation, thiophene/H_2, H_2S/H_2, H_2, and O_2; ○, (Co/Mo), ●, (S/Mo).

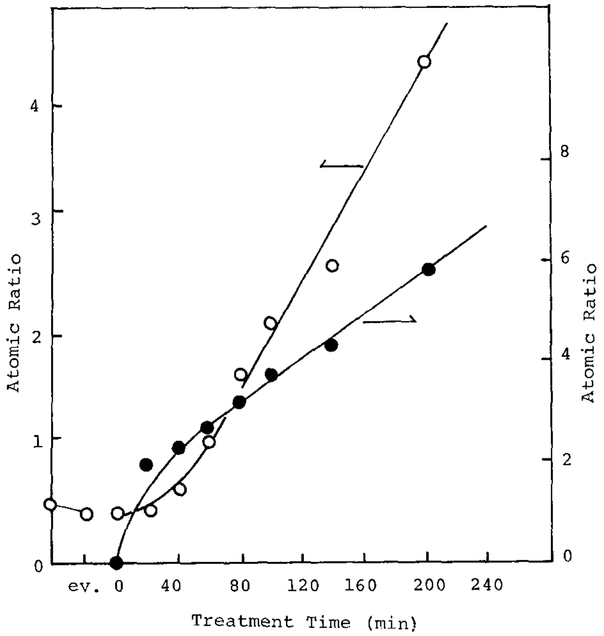

FIG. 7. Surface composition and sulfur content of the Co-Mo (B) catalyst (Co: 30 at.%) during H_2S/H_2 treatment at 400°C; ○, (Co/Mo); ●, (S/Mo).

hump observed around 227 eV in the Mo 3*d* spectrum (Fig. 2d) is due to an enhanced S 2*s* level.

The X-ray diffraction pattern of the catalyst was measured after the H_2S/H_2 treatments in Fig. 5 in order to confirm the formation of sulfided species. However, any peak indicating sulfide of molybdenum or cobalt was not detected except the diffraction peak due to MoO_2 (Fig. 4). These facts indicate that the crystallizations of the sulfided species are incomplete or only the thin surface of the catalyst is sulfided, while the catalyst is reduced completely to the bulk.

Further experiments were carried out to examine the effect of the prereduction of the catalyst. After evacuation at 400°C, 10 Torr of thiophene/H_2 was admitted to the catalyst at 400°C. As shown in Fig. 6, the (Co/Mo) ratio decreased gradually to the same level as in the case of the prereduced catalyst (Fig. 5), together with gradual increase in the (S/Mo) ratio. The effect of the prereduction of the catalyst seems to accelerate the sulfidation of the catalyst, whereas it does not change the final state of the catalyst. The successive admission of H_2S/H_2 confirmed the striking results in Fig. 5. When the sulfided catalyst was subsequently exposed to H_2, slight decreases in the (Co/Mo) and (S/Mo) ratios were observed and no change in the XPS spectra of Mo 3*d*, Co $2p_{\frac{3}{2}}$, and S 2*p* levels were detected. However, when the oxygen treatment of the catalyst was applied on the sulfided catalyst, the (Co/Mo) and (S/Mo) ratios decreased markedly (Fig. 6). Their values will reach those of the calcined catalyst by further oxidation of the sulfided catalyst. The XPS spectra of the catalyst showed again the formations of molybdenum and cobalt oxides. The S 2*p* spectrum of the O_2 treated catalyst is shown in Fig. 3f. A new peak appeared at the binding energy of 169.5 eV and it can be assigned to an oxidized sulfur, probably SO_4^{2-}, on the basis of the S 2*p* binding energy.

The oxidic catalyst was exposed to

H_2S/H_2 after evacuation at 400°C for 1 hr (Fig. 7). The remarkable increases in the (Co/Mo) and (S/Mo) ratios were observed again. When thiophene/H_2 was admitted to the catalyst sulfided by H_2S/H_2, slight decreases in the (Co/Mo) and (S/Mo) ratios were observed similar to those for the H_2 reduction of the sulfided catalyst. However, they did not reach the ratios observed in Figs. 5 and 6 where the prereduced or oxidic catalyst was treated with thiophene/H_2.

Another example is shown in Fig. 8 in order to reveal the effect of a gas composition. In this case, thiophene/H_2S/H_2 (1/1/15) was introduced to the evacuated catalyst. An intermediate behavior of the (Co/Mo) and (S/Mo) ratios was clearly observed. Therefore, these findings indicate that the surface composition and sulfur content of the catalyst depend strongly on reaction conditions employed.

Figure 9 shows the results on the surface composition and sulfur content of the catalyst when pure H_2S (10 Torr) was introduced to the catalyst at 400°C. Only a small surface segregation of cobalt was observed with a relatively high (S/Mo) ratio. Molybdenum and cobalt oxides were found to be slightly reduced.

In the case of the admission of thiophene vapor (10 Torr), the rate of formation of sulfided species was very slow ((S/Mo) was 0.17 after 60 min), accompanied by a gradual decrease in the (Co/Mo) ratio. The S 2*p* spectrum in Fig. 3e shows an appearance of a new sulfur species with ca. 2 eV-higher binding energy than that for the sulfur of sulfided molybdenum or cobalt (162.5 eV). This new sulfur can be ascribed to an adsorbed thiophene on the catalyst surface, since it was easily removed by a subsequent H_2 reduction of the catalyst, while the sulfide sulfur was not. Patterson and his co-workers (*17*) have reported similar sulfur spectrum when a prereduced Co-Mo/Al_2O_3 catalyst was exposed to thiophene vapor.

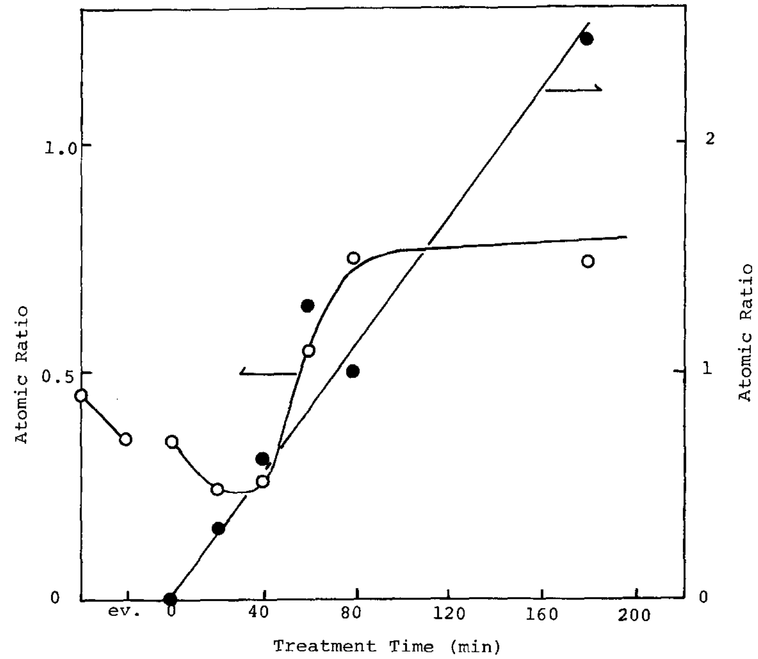

FIG. 8. Surface composition and sulfur content of the Co–Mo (B) catalyst (Co: 30 at.%) during thiophene/H_2S/H_2 treatment at 400°C; ○, (Co/Mo); ●, (S/Mo).

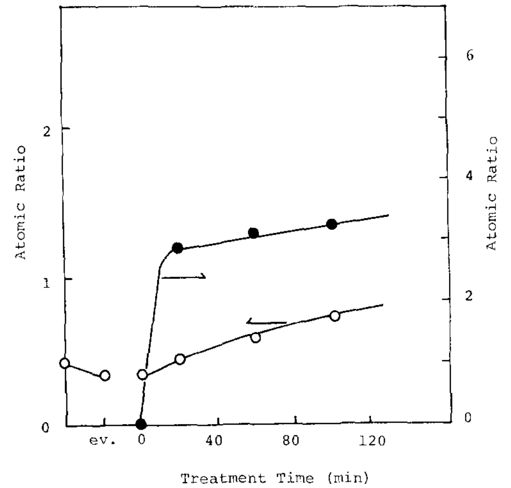

FIG. 9. Surface composition and sulfur content of the Co-Mo (B) catalyst (Co: 30 at.%) during treatment at 400°C with 10 Torr of H_2S; ○, (Co/Mo); ●, (S/Mo).

Accordingly, it is revealed that the surface composition of the Co-Mo binary oxide catalyst was changed remarkably by the contacts with the various reactive gases. The molybdenum enrichment in the catalyst surface was attained by thiophene/H_2, H_2, and thiophene vapor, whereas the superficial segregation of cobalt was accomplished by H_2S/H_2 and H_2S.

In order to reveal a driving force to cause such remarkable surface composition changes, some experiments on supported cobalt catalysts were carried out in connection with supported molybdenum catalysts (*8*). The results on the successive admissions of H_2, thiophene/H_2, and H_2S/H_2 to the cobalt catalysts (10 and 20 wt% CoO) are shown in Fig. 10. The H_2 reduction of the catalysts induced the decreases in the (Co $2p_{3/2}$/Al $2s$) XPS intensity ratio for both catalysts with a larger change for the 20 wt% catalyst than for the 10 wt% one. The XPS spectra of Co $2p_{3/2}$ level showed changes similar to those in a Co-Mo/Al_2O_3 catalyst (CoO: 3.5 wt%; MoO_3: 10 wt%) (*8*) except the larger extents of reduction in the CoO/Al_2O_3 catalysts because of the larger CoO loadings. The decreases in the (Co $2p_{3/2}$/Al $2s$) ratios can be attributed to

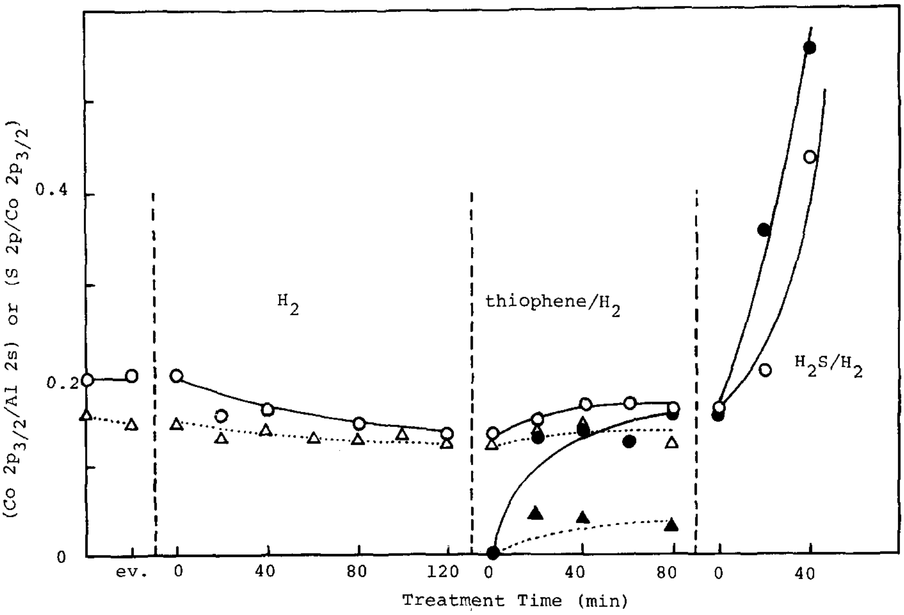

FIG. 10. Changes in the (Co $2p_{3/2}$/Al $2s$) and (S $2p$/Co $2p_{3/2}$) XPS intensity ratios for the CoO/Al_2O_3 catalysts during consecutive treatments at 400°C; H_2, thiophene/H_2, and H_2S/H_2; open symbol, (Co $2p_{3/2}$/Al $2s$); closed symbol, (S $2p$/Co $2p_{3/2}$); ○, 20 wt% CoO; △, 10 wt% CoO.

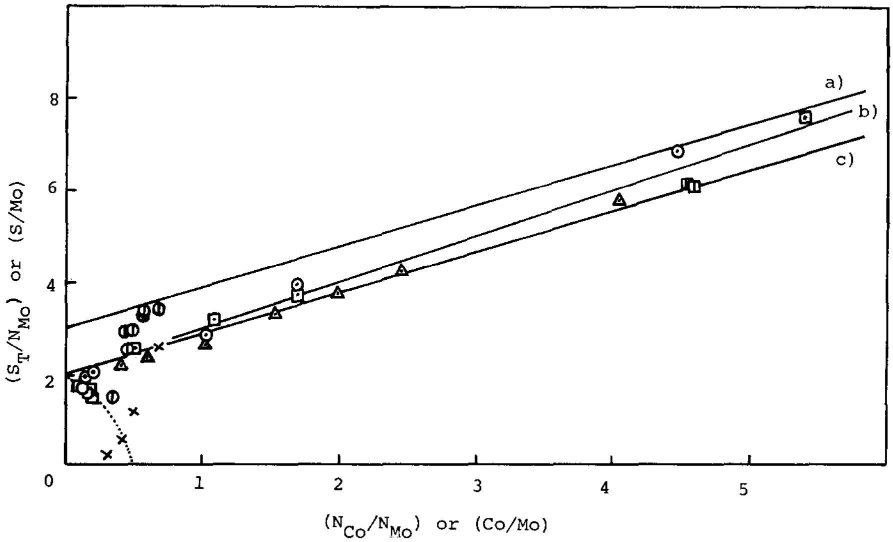

FIG. 11. Correlation between (Co/Mo) and (S/Mo) for the Co–Mo (B) catalyst (Co: 30 at.%) treated at 400°C with thiophene/H_2 (○, Fig. 5; □, Fig. 6); H_2S/H_2 (⊙, Fig. 5; ⊡, Fig. 6; △, Fig. 7); H_2 reduction after sulfidation (◫, Fig. 6), thiophene/H_2S/H_2 (×, Fig. 8); and H_2S (⦶, Fig. 9). Solid lines indicate the theoretical correlations to show the formations of (a), MoS_3 and Co_9S_8; (b), MoS_2 and CoS; and (c), MoS_2 and Co_9S_8.

the increase in the particle size of Co metal (*18–20*). The subsequent introduction of thiophene/H_2 resulted in the increases in the intensity ratio of Co and Al for both catalysts. The increases are considered to result from the migration of cobalt from the inner surface onto the outer surface of the catalyst (*8*). However, the extents of migration of cobalt onto the catalyst surfaces were considerably smaller than that of molybdenum in the MoO_3/Al_2O_3 catalyst containing a corresponding amount of supported MoO_3 (*8*). The approximate degree of sulfidation of cobalt was 0.2 for the 20 wt% CoO catalyst and much lower value was observed for the 10 wt% catalyst. These sulfur contents of the catalysts were considerably smaller than those of the MoO_3/Al_2O_3 catalysts (*8*). In the case of the H_2S/H_2 admission, great increases in the (Co $2p_{\frac{3}{2}}$/Al $2s$) and (S $2p$/Co $2p_{\frac{3}{2}}$) XPS intensity ratios were observed. Therefore, it is evident from Fig. 10 that cobalt migrates considerably onto the catalyst surface only when treated with H_2S/H_2, whereas molybdenum does so even when treated with thiophene/H_2 (*8*). Consequently, it is supposed that the surface segregation of molybdenum in the Co–Mo binary oxide catalyst is caused by the preferential interaction of molybdenum with thiophene and that the surface enrichment of cobalt is resulted from the strong interaction of cobalt with H_2S and probably from the easier diffusion of cobalt metal through the layer structure of MoS_2 or MoO_2 than those of MoS_2 and MoO_2 which are relatively fixed by the strong bonding with oxygen and sulfur. The segregation phenomena are considered to occur if a catalyst surface, even in inner pores, is accessible to reactants, although XPS informations are limited only to the outermost surface of the catalyst.

3. Sulfided States of Cobalt and Molybdenum

In the preceding section, the sulfidations of molybdenum by thiophene/H_2 and H_2S/H_2 and of cobalt by H_2S/H_2 are

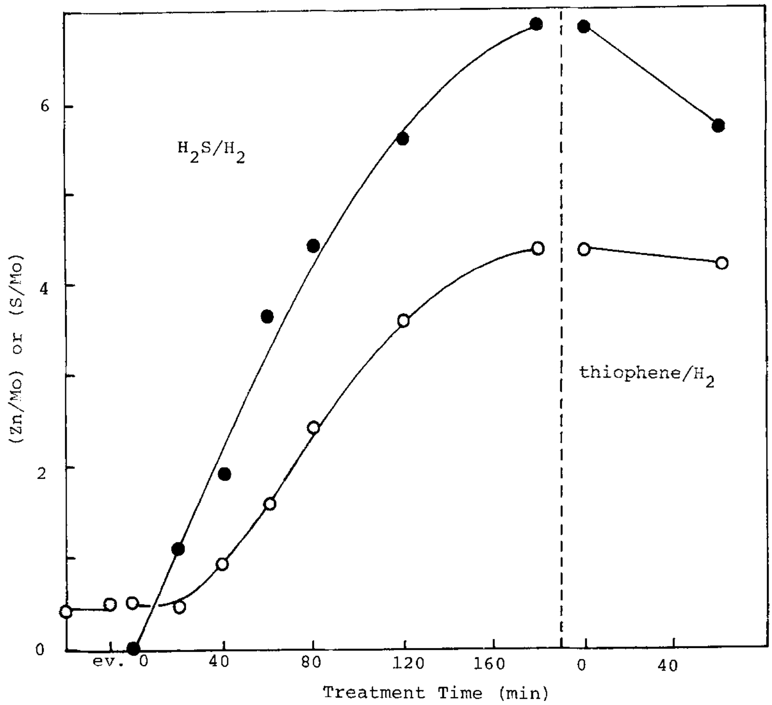

FIG. 12. Changes in surface composition and sulfur content of the Zn–Mo binary oxide catalyst (Zn: 30 at.%) during successive treatments at 400°C; evacuation, H_2S/H_2, and thiophene/H_2. ○, (Zn/Mo); ●, (S/Mo).

evident. However, there exist some sulfided forms of molybdenum and cobalt, such as MoS_2, MoS_3, CoS, Co_9S_8, and CoS_2. In this section, the results presented in Figs. 5 to 9 were analyzed more quantitatively in order to reveal the chemical states of sulfided species produced during the various treatments.

The total number of sulfur atoms in the catalyst surface, S_T, can be represented as in Eq. (1).

$$S_T = S_{Co} + S_{Mo} = (S_{Co}/N_{Co})N_{Co} + (S_{Mo}/N_{Mo})N_{Mo} \quad (1)$$

where S_{Co} and S_{Mo} are the numbers of sulfur atoms attached to Co and Mo and N_{Co} and N_{Mo} represent the atomic numbers of Co and Mo in the catalyst surface. Therefore, Eq. (2) can be derived.

$$(S_T/N_{Mo}) = (S_{Co}/N_{Co})(N_{Co}/N_{Mo}) + (S_{Mo}/N_{Mo}). \quad (2)$$

The (S_T/N_{Mo}) and (N_{Co}/N_{Mo}) ratios correspond to the (S/Mo) and (Co/Mo) in Figs. 5 to 9. Unfortunately, the respective amount of sulfur attached to cobalt (S_{Co}) or molybdenum (S_{Mo}) cannot be obtained directly from the S 2*p* XPS spectra because of the same binding energy of the S 2*p* level for both sulfides (162.5 eV). However, the (S_T/N_{Mo}) or (S/Mo) and (N_{Co}/N_{Mo}) or (Co/Mo) ratios are measurable as are shown in Figs. 5 to 9. If certain stoichiometric sulfide species are formed by the preceding treatments, linear correlations are anticipated between the (S/Mo) and (Co/Mo) ratios. The following equations can be obtained, provided the sulfide species having stoichiometric compositions are formed;

for MoS_2 and CoS:

$$(S/Mo) = 1 \times (Co/Mo) + 2; \quad (3)$$

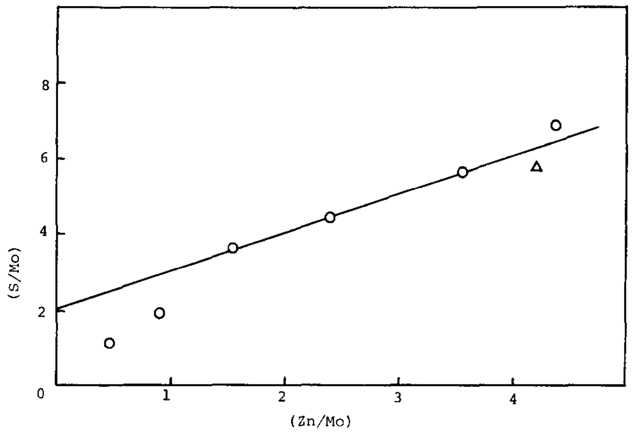

FIG. 13. Correlation between (Zn/Mo) and (S/Mo) for the Zn–Mo catalyst (Zn: 30 at.%) at 400°C with H_2S/H_2 (○) and subsequently with thiophene/H_2 (△). Solid line indicates the theoretical correlation for MoS_2 and ZnS formations.

for MoS_2 and Co_9S_8:

$$(S/Mo) = (8/9) \times (Co/Mo) + 2; \quad (4)$$

for MoS_3 and Co_9S_8:

$$(S/Mo) = (8/9) \times (Co/Mo) + 3. \quad (5)$$

The solid lines (a), (b), and (c) in Fig. 11 correspond to the above theoretical correlations, that is, to Eqs. (5), (3), and (4), respectively. The (S/Mo) ratio was replotted in Fig. 11 as a function of the (Co/Mo) ratio, whereas these ratios are plotted against the treatment time in Figs. 5 to 9.

In the cases of the thiophene/H_2 treatments of the reduced catalyst (Fig. 5) and of the catalyst evacuated at 400°C (Fig. 6), experimental data approach gradually to the point (S/Mo) = 2 along the dotted line in Fig. 11, as the (Co/Mo) ratio decreases or as the treatment time becomes longer. However, when the catalyst is treated with H_2S/H_2, the (S/Mo) ratio correlates very well to the theoretical line (b) or (c), particularly in the region where the (Co/Mo) ratio does not exceed about 4, indicating the formations of stoichiometric compounds: MoS_2 and CoS and/or Co_9S_8. Somewhat higher (S/Mo) ratios were obtained for the catalyst with higher (Co/Mo) ratios, that is, for the catalysts exposed to H_2S/H_2 for a prolonged time. After the H_2 reduction of the sulfided catalyst (Fig. 6), the (S/Mo) ratio becomes to fit line (c) completely. With regard to the H_2S treatments, the (S/Mo) ratio is considerably higher than that expected from the theoretical line (b) or (c). From these findings, the following conclusions can be drawn: (1) the thiophene/H_2 treatments preferentially sulfide molybdenum to produce MoS_2 as expected from the (S/Mo) ratios in Figs. 5 and 6; (2) the H_2S/H_2 admission results in the sulfidation of molybdenum and cobalt and produces MoS_2 and CoS and/or more likely Co_9S_8; and (3) the prolonged H_2S/H_2 and pure H_2S treatments cause excess sulfur on the catalyst surface, which can be removed very easily by the reduction with H_2. In the case of the pure H_2S treatments at 400°C, MoS_3, which consists of subcrystalline MoS_2 and excess amorphous sulfur (*21*), might be produced, because the corresponding points seem to approach to line (a). With regard to the admission of thiophene/H_2S/H_2, the experimental data approach line (c) in a manner intermediate between the H_2S/H_2 and thiophene/H_2 treatments, indicating simultaneous sulfidations of both cobalt and molybdenum unstoichiometrically in its initial stage. These analyses proved XPS technique to be very powerful for the determination of surface species in complicated systems.

4. Zinc–Molybdenum Binary Oxide Catalyst

ZnO–MoO_3 binary oxide catalysts were studied for comparison with the Co–Mo binary oxide catalysts, since ZnO has been reported to be a good promoter as CoO for the hydrodesulfurization of thiophene (*22*). In Fig. 12, the (Zn/Mo) and (S/Mo) atomic ratios of the Zn–Mo catalyst (Zn/Zn + Mo = 0.3) are shown during successive treatments with H_2S/H_2 and thiophene/H_2. Similar behavior was observed as in the case of the Co–Mo catalyst. A considerable surface enrichment of zinc was observed for the H_2S/H_2 treatments, and the (Zn/Mo) and (S/Mo) ratios were decreased as mentioned for the Co–Mo catalyst when the sulfided catalyst was exposed to thiophene/H_2. The binding energy of Zn $2p_{\frac{3}{2}}$ level shifted from 1022.5 to 1022.1 eV and the kinetic energy of Zn $L_3M_{4,5}M_{4,5}$ (^1G) Auger peak changed from 985.1 to 986.3 eV during the H_2S/H_2 treatments. These shifts are in good agreement with those expected for the sulfidation of ZnO to ZnS (*23*). The H_2 reduction and thiophene/H_2 treatments of the Zn–Mo catalyst caused the decrease in the (Zn/Mo) ratio, but produced no Zn metal, on the contrary to the Co metal formation in the Co–Mo catalyst.

A similar quantitative analysis (Fig. 13) as in Fig. 11 for the Co–Mo catalyst shows the formation of ZnS and MoS_2, together with a possible excess sulfur production by the prolonged treatment with H_2S/H_2.

CONCLUSIONS

The surface compositions of the calcined Co–Mo binary oxide catalysts, which were prepared by calcining the mixtures of cobaltous nitrate and ammonium paramolybdate, are considerably different from the bulk compositions. The surface enrichment of molybdenum was found in the catalysts which contain cobalt more than about 6 at.%. In the composition range of a small content of cobalt, cobalt was slightly enriched in the catalyst surface. However, in the cases of the Co–Mo catalysts, which were prepared by the calcination of the mixed composite oxides, no appreciable difference between surface and bulk compositions was detected except the catalyst containing a small amount of cobalt where the cobalt enrichment was observed.

The drastic changes in the surface composition of the Co–Mo catalyst were found during a variety of treatments at 400°C with 10 Torr of gases relating to the hydrodesulfurization of thiophene. Thiophene/H_2 and H_2 caused the surface segregation of molybdenum, whereas cobalt was markedly enriched by H_2S/H_2. Thiophene/H_2 produced preferentially MoS_2, and H_2S/H_2 formed MoS_2 and CoS and/or more likely Co_9S_8, accompanied by excess sulfur. The Zn–Mo binary oxide catalyst showed similar behavior to that of the Co–Mo catalyst in the changes of the surface composition during the treatments.

It is clearly demonstrated that the surface composition and sulfur content of the catalyst depend remarkably on the preparation method and on the kind and period of the treatment and that the quantitative analysis of XPS spectra is effective to define surface composition and surface species. Although various catalytic reactions have been conducted on multicomponent catalysts, only a little attention has been paid on the surface compositions of the oxide catalysts so far. Our results strongly suggest that more considerations on the surface composition of the catalyst under reaction conditions are needed to discuss catalytic properties in detail such as activity, selectivity, and promoter effect, as suggested previously (*7*).

REFERENCES

1. Ponec, V., *Catal. Rev.* **11**, 1 (1975).
2. Sinfelt, J. H., *Accounts Chem. Res.* **10**, 15 (1977).
3. Overbury, S. H., Ertrand, P. A., and Somorjai, G. H., *Chem. Rev.* **75**, 547 (1975).
4. Matsuura, I., and Wolfs, M. W. J., *J. Catal.* **37**, 174 (1975).
5. Grzybowska, B., Haber, J., Marczewski, W., and Ungier, L., *J. Catal.* **42**, 327 (1976).
6. Prasada Rao, T. S. R., and Menon, P. G., *J. Catal.* **51**, 64 (1978).
7. Okamoto, Y., Hashimoto, T., Imanaka, T., and Teranishi, S., *Chem. Lett.* 1035 (1978).
8. Okamoto, Y., Nakano, H., Shimokawa, T., Imanaka, T., and Teranishi, S., *J. Catal.* **50**, 447 (1977).
9. Frost, D. C., McDowell, C. A., and Woosley, I. S., *Mol. Phys.* **27**, 1473 (1974).
10. Okamoto, Y., Nakano, H., Imanaka, T., and Teranishi, S., *Bull. Chem. Soc. Japan* **48**, 1163 (1975).
11. Chuang, T. G., Brundle, C. R., and Rice, D. W., *Surface Sci.* **59**, 413 (1976).
12. Canesson, P., Delmon, B., Delvaux, G., Grange, P., and Zabala, J. M., *in* "Proceedings, 6th Int. Congr. Catal., London, 1976," B32.
13. Imanaka, T., Sakurai, K., Hashimoto, T., Okamoto, Y., and Teranishi, S., unpublished results.
14. Wheeler, A. M., and Bettman, M., *J. Catal.* **40**, 124 (1975).
15. Defosse, C., Canesson, P., Rouxhet, P. G., and Delmon, B., *J. Catal.* **51**, 209 (1978).
16. Hagenbach, G., Courty, P., and Delmon, B., *J. Catal.* **31**, 264 (1973).
17. Patterson, T. A., Carver, J. C., Leyden, D. C., and Hercules, D. M., *J. Phys. Chem.* **80**, 1700 (1976).
18. Escard, J., Pontivianne, B., Chenebaux, M. T., and Cosyns, J., *Bull. Soc. Chim. Fr.* 349 (1976).
19. Brinen, J. S., Schmitt, J. L., Dougham, W. R., Achorn, P. J., Siegel, L., and Delgass, W. N., *J. Catal.* **40**, 295 (1975).
20. Angevine, P. J., Delgass, W. N., and Vartuli, J. C., *in* "Proceedings, 6th Int. Congr. Catal., London, 1976," B1.
21. Stevens, G. C., and Edmonds, T., *J. Catal.* **37**, 544 (1975).
22. deBeer, V. H. J., Van Sint Fiet, T. H. M., Engelen, J. F., Van Haadel, A. C., Wolfs, M. W. J., Amberg, C. H., and Schuit, G. C. A., *J. Catal.* **27**, 357 (1972).
23. Nishikida, S., and Ikeda, S., *Bull. Chem. Soc. Japan* **51**, 154 (1978).